

# Confocal Ellipse-based Distance and Confocal Elliptical Field for polygonal shapes

Aysylu Gabdulkhakova

Pattern Recognition and Image Processing group  
Technische Universität Wien  
Favoritenstrasse 9-11, Vienna, Austria  
Email: aysylu@prip.tuwien.ac.at

Walter G. Kropatsch

Pattern Recognition and Image Processing group  
Technische Universität Wien  
Favoritenstrasse 9-11, Vienna, Austria  
Email: krw@prip.tuwien.ac.at

**Abstract**—The paper introduces a novel confocal ellipse-based distance (CED), that is based on the properties of the confocal ellipses. This distance is used to produce a confocal elliptical field (CEF). The Euclidean Distance Transform (EDT) of a single point (called seed) generates a distance field of concentric circles. The sum of two such distance fields of two distinct seed points produces a distance field of confocal ellipses. This fact enables to adapt CED and CEF to the discrete case, referred to as CED-DT and CEF-DT. The properties of the CEF and CEF-DT make them useful for skeletonization, in particular for efficient removal of the spurious branches.

## I. INTRODUCTION

Distance Transform (DT) [1] is an operator that assigns to every point its shortest distance to the seed point set in terms of a particular distance function. In scopes of image processing, such distances can encode spatial information (e.g. distance to the boundary of the shape), or characteristic information (e.g. distance between the features) [2].

In shape analysis, Euclidean DT (EDT) is of special interest, since it is invariant under rotation, translation, and bending in 2D, but not under scaling. Related methods work with the data on a grid (pixels in 2D, and voxels in 3D). Given a binary image, EDT computes for each pixel of a shape its shortest distance to the background. The algorithm that computes the exact EDT in linear time was proposed by Maurer et al. [3], and later improved by Ciesielski et al. [4].

To the best of our knowledge, there exist no algorithm for producing a distance field of a polygonal shape using confocal ellipses. Talbot et al. [5] presented an Elliptical Distance Transform (LDT) for the problem of splitting the overlapping disk-like shapes. The approach aims at reducing the dimensionality of the ellipse fitting problem by using the series of distance transforms, and optimizing the eccentricity and orientation parameters of the ellipses. In contrast, this paper is targeting the polygonal shapes. It introduces a distance function and a distance field that are based on properties of the confocal ellipses.

The areas of DT application include, but are not limited to image matching, image segmentation, object recognition, and shape analysis. In particular, DT provides a basis to skeletonization approaches, which in turn is a widely exploited shape descriptor in a vast number of domains [6].

Skeletonization is the process of obtaining a compact one-pixel wide shape representation, called skeleton. The skeleton of a shape is primarily associated with the medial axis transform (MAT) introduced by Blum [7]. By definition MAT is a locus of centers of circles tangent to the boundary in at least two distinct points. As a shape descriptor, MAT has the following properties: (1) it is invariant to translation, rotation, scaling; (2) it preserves symmetry and local thickness of the shape; (3) it can be computed for any 2D shape; (4) it incorporates adjacency and neighborhood information; (5) original shape can be completely reconstructed from MAT. Existing skeletonization approaches can be generally classified as digital and continuous [8].

Continuous approaches consider analytical computation of the skeleton given an approximation of the shape boundary. A group of methods is derived from the Voronoi diagram [9]. These methods take all the boundary pixels as seeds. They preserve topological, as well as geometrical information about the shape. The skeleton is considered to be a subset of the Voronoi diagram, that excludes the bisectors of the incident seeds, and the points of the remaining bisectors that do not belong to the given shape. The size of the seed set has a crucial influence on computational efficiency of the approach. Therefore, the methods from this category aim to find a trade-off between the accuracy of the skeleton and the computational costs [10]–[12]. Another group of continuous methods is based on the principle of continuous curve evolution [13]–[15]. In particular, Kimmel et al. [13] proposed an approach that decomposes a shape boundary into segments, for which EDT can be computed in parallel. A skeleton is then obtained as a set of points, where multiple distance fields share the same value. In case every point of the boundary represents a segment, the algorithm produces the Voronoi diagram. These properties are also valid for the proposed confocal elliptical field. The difference is, that the produced skeleton in its general form consists of hyperbolic curves instead of bisectors. Though, as a special case, it creates the Voronoi diagram.

An important drawback of digital and continuous approaches is its sensitivity to noise: small perturbations along the border of the shape cause spurious branches in the resulting skeleton. To solve this problem, several solutions were proposed, including boundary smoothing, polygonal approxi-

mation of the shape, hierarchy of skeletons, weighting of the seed points [16].

This paper introduces an approach, that takes the pairs of successive points of the shape border as focal points of the ellipse, and generates a new type of the distance field - confocal elliptical field (CEF). The CEF provides the basis for a continuous skeletonization approach, where the separating curves are represented by branches of hyperbolas. In a specific case, when the distances between the focal points of all ellipses are the same, the hyperbolas degenerate into bisectors. In particular, when every point of the shape border represents an ellipse degenerated into a circle, the method produces a Voronoi diagram. Thus, the proposed approach can be considered as a generalization of the Voronoi diagram. The methodology presented in this paper opens new possibilities for shape analysis.

The contributions are as follows:

- a confocal ellipse-based distance is introduced, and formally defined for continuous (CED) and discrete cases (CED-DT);
- a confocal elliptical field is introduced and formally defined for continuous (CEF) and discrete case (CEF-DT);
- discussion of the properties of CEF and CEF-DT that are useful for the problem of skeletonization.

The remaining of the paper is organized as follows. Section 2 and Section 3 introduce confocal ellipse-based distance (CED) and confocal elliptical field (CEF) respectively. The methods for computing CED and CEF on a digital grid, CED-DT and CEF-DT correspondingly, are discussed in Section 4. The properties of CEF and CEF-DT that are useful for skeletonization are given in Section 5. Finally, Section 6 concludes the paper.

## II. CONFOCAL ELLIPSE-BASED DISTANCE (CED)

Let  $d(M, N) = \sqrt{(x_M - x_N)^2 + (y_M - y_N)^2}$ ,  $M, N \in \mathbb{R}^2$ , be the Euclidean distance between the points  $M$  and  $N$ .

**Definition 1.** *The ellipse  $E(F_1, F_2; a)$  is the locus of points  $P \in \mathbb{R}^2$  on a plane, for which the sum of the distances to two given points  $F_1$  and  $F_2$  (called focal points) is constant:*

$$E(F_1, F_2; a) = \{ P \in \mathbb{R}^2 \mid d(P, F_1) + d(P, F_2) = 2a \} \quad (1)$$

Here  $a \geq f = \frac{1}{2}d(F_1, F_2)$  is the length of the semi-major axis of the ellipse, and  $f$  is half the distance between the focal points. In case  $a = f$ , the ellipse degenerates into a line segment.

**Definition 2.** *Ellipses that have the same focal points  $F_1$  and  $F_2$  are called confocal ellipses.*

For confocal ellipses we use the simplified notation that depends only on a parameter  $a$ , i.e.  $E(a) = E(F_1, F_2; a)$ . A family of confocal ellipses covers the whole plane:

$$\bigcup_{a=f}^{\infty} E(a) = \mathbb{R}^2 \quad (2)$$

It means that for any point  $P \in \mathbb{R}^2$  on a plane, there is a unique ellipse  $E(F_1, F_2; a)$  that passes through it [17]. This property enables to consider the value of  $a$  as the distance from  $P$  to the line segment  $\overline{F_1 F_2}$ .

**Definition 3.** *Let  $E(a_1)$  and  $E(a_2)$  be confocal ellipses. The confocal ellipse-based distance (CED),  $e : \mathbb{R}^2 \times \mathbb{R}^2 \rightarrow \mathbb{R}$ , is the absolute difference between the lengths of the semi-major axes  $a_1$  and  $a_2$  of these ellipses:*

$$e(E(a_1), E(a_2)) = |a_1 - a_2| \quad (3)$$

CED is a metric, and  $E(a_1) \supset E(a_2)$ , if  $a_1 > a_2$ .

## III. CONFOCAL ELLIPTICAL FIELD (CEF)

Consider a line segment  $\overline{F_1 F_2}$  between the points  $F_1$  and  $F_2$ . In analogy to the EDT which generates distances from points, we now use the line segment as seed  $s = (F_1, F_2)$  and generate the distance  $a_P$  of a point  $P \in \mathbb{R}^2$  such that  $P \in E(F_1, F_2; a_P)$  according to Equation (1). The distance  $c(P, s)$  from the point  $P$  to the line-seed  $s$  is defined by CED as:

$$c(P, s) = e(E(a_P), E(a_0)), \quad (4)$$

where  $E(a_P)$  corresponds to the unique ellipse with focal points  $F_1$  and  $F_2$  that contains  $P$ ;  $E(a_0)$  corresponds to the ellipse with the same foci  $F_1$  and  $F_2$ , that degenerated into a line segment. In other words, this distance is equal to:  $c(P, s) = d(P, F_1) + d(P, F_2) - d(F_1, F_2) = 2(a_P - f)$ .

Consider now a finite set of line-seeds defined by the pairs of end points:  $S = \{(F_1, F_2), (F_2, F_3), \dots, (F_N, F_{N+1})\}$ . Every seed  $s_i = (F_i, F_{i+1})$ ,  $i \in [1, \dots, N]$  generates a family of confocal ellipses. Any point  $P \in \mathbb{R}^2$  has a distance  $d(P, s_i)$  to every seed  $s_i$  of which the closest determines the distance to the complete set of seeds:

**Definition 4.** *The confocal elliptical field (CEF) assigns to each point  $P \in \mathbb{R}^2$  its distance to the closest seed from  $S$ :*

$$CEF = c(P, S) = \inf \{ c(P, s_i) \mid s_i \in S, i \in [1, \dots, N] \} \quad (5)$$

A CEF combines the distances of the different line-seeds and partitions  $\mathbb{R}^2$  into cells that contain the shortest distance to a single seed (similar to Voronoi cells).

**Definition 5.** *A separating curve separates the receptive fields of two different line-seeds.*

Let us consider a few special cases of two pairs of line-seeds. In this case, the separating curve is either a bisector, or a branch of a hyperbola. Let  $P \in \mathbb{R}^2$  be a point on a separation curve.

- 1) Two degenerated seeds  $S = \{(F_1, F_1), (F_2, F_2)\}$ :  
 $2d(P, F_1) - d(F_1, F_1) = 2d(P, F_2) - d(F_2, F_2)$   
 In this case the separating curve is a bisector of  $\overline{F_1 F_2}$ :  
 $d(P, F_1) = d(P, F_2)$  (see Fig. 2b).
- 2) Two consecutive line-seeds  $S = \{(F_1, F_2), (F_2, F_3)\}$  with equal length, i.e.  $d(F_1, F_2) = d(F_2, F_3)$ :  
 $d(P, F_1) + d(P, F_2) - d(F_1, F_2) =$   
 $d(P, F_2) + d(P, F_3) - d(F_2, F_3)$

As in the previous case, the separation curve is a bisector:  $d(P, F_1) = d(P, F_3)$  (Fig. 4a).

- 3) Two consecutive line-seeds  $S = \{(F_1, F_2), (F_2, F_3)\}$ , with  $d(F_1, F_2) \neq d(F_2, F_3)$ . Re-arranging the terms we get  $d(P, F_1) - d(P, F_3) = d(F_1, F_2) - d(F_2, F_3)$ . The resulting equation defines a branch of the hyperbola with the focal points  $F_1$  and  $F_3$ , which passes through the point  $F_2$  (Fig. 4b).

The tangent to the hyperbola at any point  $F_2 \in \mathfrak{R}^2$ ,  $F_2 \notin F_1F_3$ , bisects the angle  $\widehat{F_1F_2F_3}$ . In this manner, when  $d(F_1, F_2) = d(F_2, F_3)$ , the hyperbola degenerates into a bisector (see Fig. 4a).

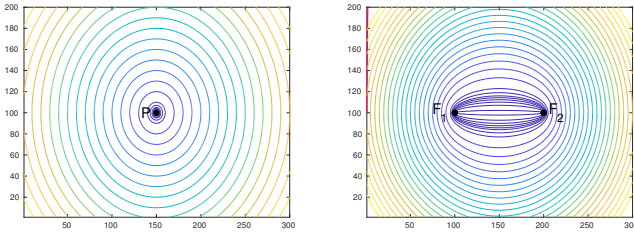
#### IV. CED AND CEF IN TERMS OF DISTANCE TRANSFORM

Since in image processing the algorithms are working on a digital grid, let us in this section adapt the proposed continuous methods for the discrete case using the DT.

**Definition 6.** Given a set of point-seeds  $S \in B = [0, n] \times [0, m] \subset \mathbb{Z}^2$ , the distance transform (DT) obtains a gray-scale distance field  $D : B \mapsto \mathfrak{R}$ . The intensity value of each pixel  $D(p) = \min\{d(p, s) | s \in S\}$  equals the distance to the nearest seed in accordance to the selected metric.

The DT can be computed using various metrics, e.g. Euclidean, Chessboard, or City-Block [18]. The Euclidean distance is invariant under rotation, translation, and bending in 2D, but not under scaling. These properties make it useful for the shape description and representation. In this paper the distance field  $D$  is considered to be the result of DT with Euclidean metric.

Let  $D_P$  be the distance field that is generated for the seed set with a single pixel  $P \in B$ . The contour lines of this field are concentric circles (Fig. 1a). Let  $D_P(M)$  be the distance value at pixel  $M \in B$ . Then,  $D_P(M) = d(M, P) \geq 0$ .



(a) concentric circles (b) confocal ellipses

Fig. 1: Distance fields represented by isolines

Let us refine the Definition 2 (confocal ellipses), Definition 3 (CED), and Definition 4 (CEF) for the discrete case using the DT.

**Definition 7.** Consider the line-seed  $S = \{(F_1, F_2)\}$  of two pixels. Confocal ellipses can be obtained as a sum of distance fields generated from  $F_1$  and  $F_2$ :

$$C_{F_1F_2} = D_{F_1} + D_{F_2} \quad (6)$$

The pixel-wise sums are independent on the order of execution and can be computed in a single parallel step. According to Definition 7, the intensity value of pixel  $P \in C_{F_1F_2}$  equals the length of the semi-major axis  $a$  of the unique ellipse with foci  $F_1$  and  $F_2$  that contains  $P$  (see Fig. 1b). This fact was also mentioned by Strand [19]. In contrast, CED that is used in CEF defines the absolute difference between  $a$  and  $d(F_1, F_2)$  (see Definition 3). With this regard, let us provide a definition that is compliant to CED.

**Definition 8.** Consider the seed set  $S = \{F_1, F_2\}$  that has two pixels, and the corresponding distance field of confocal ellipses  $C_{F_1F_2}$ . The distance field  $\overline{C}_{F_1F_2}$ , where the intensity value of each pixel  $P$  denotes its CED with respect to focal points  $F_1$  and  $F_2$  is computed as:

$$\begin{aligned} \overline{C}_{F_1F_2}(P) &= C_{F_1F_2}(P) - C_{F_1F_2}(F_1) \\ &= C_{F_1F_2}(P) - C_{F_1F_2}(F_2) \\ &= D_{F_1}(P) + D_{F_2}(P) - D_{F_1}(F_2) \\ &= D_{F_1}(P) + D_{F_2}(P) - D_{F_2}(F_1) \end{aligned} \quad (7)$$

The distance field  $\overline{C}_{F_1F_2}$  also contains confocal ellipses. In contrast to  $C_{F_1F_2}$ , the intensity values of its pixels are independent from the distance between the focal points  $F_1$  and  $F_2$ . This fact enables to combine multiple distance fields of such type, and find, for example, the minimum CED value for each pixel. In general, the distance field  $\overline{C}_{F_1F_2}$  has the following related properties:

- 1) The distance value at the seed pixel of  $D$  is zero:  $D_{F_1}(F_1) = D_{F_2}(F_2) = 0$
- 2) Given two distance fields  $D_{F_1}$  and  $D_{F_2}$  with seeds  $F_1 \neq F_2$  correspondingly, the distance of the opposite seeds is the same:  $D_{F_1}(F_2) = D_{F_2}(F_1) = d(F_1, F_2)$
- 3) In distance field  $\overline{C}_{F_1F_2}$ , generated by a line-seed of pixels  $F_1$  and  $F_2$ , the distance values along the discrete line segment  $\overline{F_1F_2}$  are close to zero:  $\overline{C}_{F_1F_2}((1 - \lambda)F_1 + \lambda F_2) < \epsilon < \sqrt{2}/2, \forall \lambda \in [0, 1]$ .

**Definition 9.** Let  $S = \{(F_1, F_2), (F_2, F_3), \dots, (F_N, F_{N+1})\}$  be a set of line-seeds, and  $\overline{C} = \{\overline{C}_{F_1F_2}, \overline{C}_{F_2F_3}, \dots, \overline{C}_{F_NF_{N+1}}\}$  be the corresponding CED distance fields. The confocal elliptical field in terms of DT (CEF-DT) is computed by pixel-wise minimum operation applied to the distance fields of  $\overline{C}$ :

$$CEF_{DT}(P) = \min\{\overline{C}_{F_i, F_{i+1}}(P) \mid i = 1, \dots, N\} \quad (8)$$

Notice that also this operation can be executed in parallel for all seeds. In this paper the target shape is polygonal. Let us now consider several specific cases of CEF-DT.

A. Two point-seeds, i.e.  $S = \{(F_1, F_1), (F_2, F_2)\}$ .

The CEF-DT is equal to  $CEF_{DT} = \min(\overline{C}_{F_1F_1}, \overline{C}_{F_2F_2})$ , for all pixels of the image. As follows from the discussion in Section III,  $\overline{C}_{F_1, F_1}$  and  $\overline{C}_{F_2, F_2}$  are separated by a bisector (see Fig. 2a). Indeed, with relation to Definition 5:

$$\begin{aligned} \overline{C}_{F_1, F_1} = \overline{C}_{F_2, F_2} &\Leftrightarrow 2D_{F_1} = 2D_{F_2} \Leftrightarrow \\ &\Leftrightarrow d(P, F_1) = d(P, F_2), \forall P \in \text{separating curve} \end{aligned} \quad (9)$$

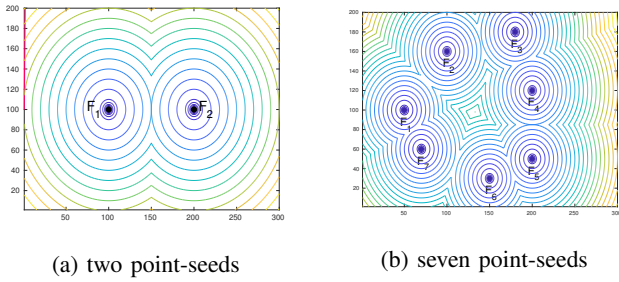


Fig. 2: CEF-DT for point-seeds

In general, for  $N > 1$  consecutive seeds, the resulting field contains  $N$  fields separated by bisectors. In this case, the final representation is a Voronoi diagram (see Fig. 2b).

### B. Two successive line-seeds $S = \{(F_1, F_2), (F_2, F_3)\}$ .

The CEF-DT equals  $CEF_{DT}(P) = \min\{\overline{C}_{F_1F_2}, \overline{C}_{F_2F_3}\}$ . As follows from the discussion in Section III,  $\overline{C}_{F_1F_2}$  and  $\overline{C}_{F_2F_3}$  are separated by a branch of a hyperbola (see Fig. 3a). Indeed,  $D_{F_1} - D_{F_3} = D_{F_2}(F_1) - D_{F_2}(F_3)$  is a constant and equals the difference between  $d(F_1, F_2)$  and  $d(F_2, F_3)$ . The difference  $D_{F_1} - D_{F_3}$  defines a branch of a hyperbola with focal points  $F_1$  and  $F_3$  that passes through the common pixel  $F_2$  (see Fig. 3b).

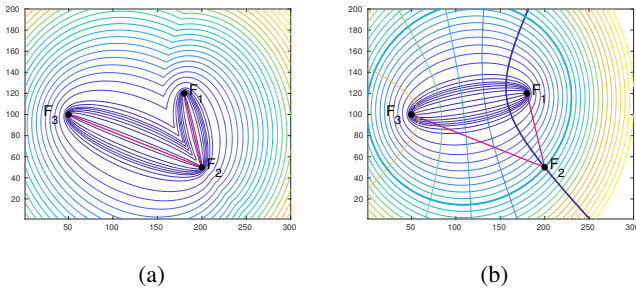


Fig. 3: (a) CEF-DT for  $S = \{(F_1, F_2), (F_2, F_3)\}$  (b) confocal hyperbolas with focal points at  $F_1$  and  $F_3$

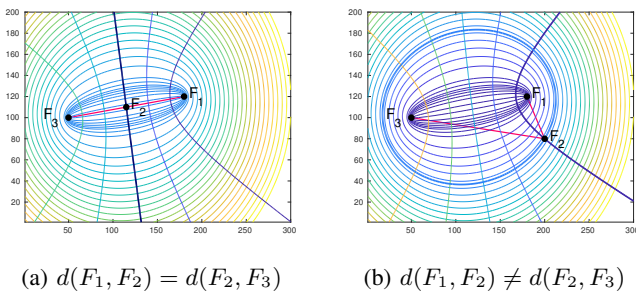


Fig. 4: Change of the hyperbola curvature due to the position of the common point  $F_2$  in two given line segments

In the continuous case, the focal points  $F_1$  and  $F_3$  can be used to generate a set of hyperbolas that covers the given plane [17]. As well as for confocal ellipses, each point  $P \in \mathbb{R}^2$

is contained only in one hyperbola from the set. Therefore, given a pair of line segments  $(F_1, F_2)$  and  $(F_2, F_3)$ , the separating curve between them is a unique branch of the hyperbola, generated by focal points  $F_1$  and  $F_3$ , that passes through the point  $F_2$ . The position of  $F_2$  defines the curvature of the hyperbola (see Fig. 4).

### C. Closed polygon $S = \{(F_1, F_2), (F_2, F_3), \dots, (F_N, F_1)\}$ .

The CEF-DT is computed as  $CEF_{DT}(P) = \min\{\overline{C}_{F_1, F_2}, \overline{C}_{F_2, F_3}, \dots, \overline{C}_{F_{N-1}, F_N}, \overline{C}_{F_N, F_1}\}$ . With the reference to Equation (5), the CEF-DT contains  $N$  fields, with  $N$  separating hyperbolas that pass through the vertices of the polygon. The other separating curves may have inflection points and are only defined implicitly in this paper. All hyperbolas do not necessarily intersect at the same point, though taking the minimum at each point  $P$ , creates the separation curve in the zones of similar influence of more than one CED-based distance fields (see the example in Fig. 5).

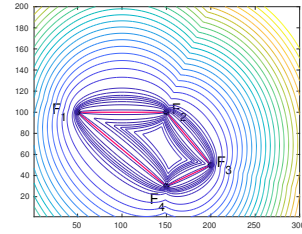


Fig. 5: CEF-DT of the closed polygon defined by four pairs of pixels  $S = \{(F_1, F_2), (F_2, F_3), (F_3, F_4), (F_4, F_1)\}$

## V. PROPERTIES OF THE CEF AND CEF-DT

### A. Receptive field of a line-seed

Consider a set of seeds  $S = \{s_1, s_2, \dots, s_N\}$ . Let the receptive field (or alternatively the Voronoi-cell)  $R_i \subset \mathbb{R}^2$  of the seed  $s_i \in S$ ,  $i \in [1, \dots, N]$  denote a set of points in CEF for which the CED to  $s_i$  is smaller than to any other seed  $s_j \in S$ ,  $j \in [1, \dots, N], j \neq i$ . In the continuous case, with the reference to Equation (4) and Equation (5) the receptive field  $R_i$  can be computed as:

$$R_i = \{CEF(P) - d(P, s_i) = 0 \mid P \in \mathbb{R}^2, i \in [1, \dots, N]\}$$

Correspondingly, in the discrete case, with the seed  $s_i = (F_p, F_q)$ ,  $p, q \in [1, \dots, M]$  with the reference to Equation (7) and Equation (8):

$$R_i = \{CEF_{DT} - \overline{C}_{F_p F_q} \leq \epsilon \mid i \in [1, \dots, N]\}$$

Here  $\epsilon$  is a value that is close to zero and aims at handling the discretization errors.

### B. Seeds that belong to the same line

**Theorem 1.** Let  $F_1, F_2, F_3, F_4$  be consecutive points that belong to the same line. If the seed set contains the pairs of points  $S = \{(F_1, F_4), (F_2, F_3)\}$ , the resulting CEF contains only the CED values generated by the line-seed  $(F_1, F_4)$ .

*Proof.* Let  $P \in \mathbb{R}^2$  be an arbitrary point in a plane. Let us prove that:

$$\begin{aligned} d(P, F_1) + d(P, F_4) - d(F_1, F_4) &\leq \\ &\leq d(P, F_2) + d(P, F_3) - d(F_2, F_3) \end{aligned} \quad (10)$$

Since  $F_2$  and  $F_3$  are between  $F_1$  and  $F_4$  on the same line, then:  $d(F_1, F_4) = d(F_1, F_2) + d(F_2, F_3) + d(F_3, F_4)$ . Substituting  $d(F_1, F_4)$  in Equation (10) and re-arranging:

$$\begin{aligned} d(P, F_1) + d(P, F_4) - d(F_1, F_2) - d(F_3, F_4) &\leq \\ &d(P, F_2) + d(P, F_3) \\ d(P, F_1) + d(P, F_4) - d(P, F_2) - d(P, F_3) &\leq \\ &d(F_1, F_2) + d(F_3, F_4) \\ (d(P, F_1) - d(P, F_2)) + (d(P, F_4) - d(P, F_3)) &\leq \\ &d(F_1, F_2) + d(F_3, F_4) \end{aligned}$$

With regard to the triangle inequality,

$$d(F_1, F_2) \geq |d(P, F_1) - d(P, F_2)|$$

$$d(F_3, F_4) \geq |d(P, F_3) - d(P, F_4)|$$

Therefore, Equation (10) is true.  $\square$

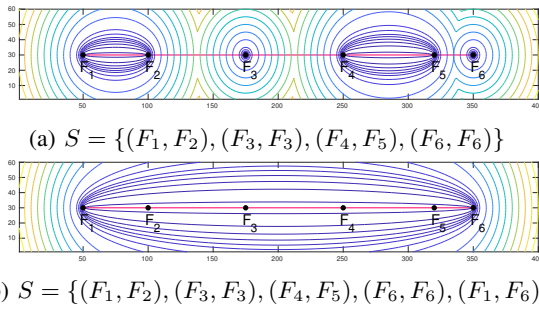


Fig. 6: CEF-DT for the seed pixels that lie on the same line.

The same holds true in the discrete case. The resulting CEF-DT will be equal to  $\bar{C}_{F_1, F_4}$ . An example is shown in Fig. 6. The receptive fields of the seeds that correspond to the line segment (see Fig. 6a) are fully absorbed by the receptive field of its end points  $F_1$  and  $F_6$  (see Fig. 6b).

### C. Skeletonization

In this paper the target shape is polygonal. Approximations of objects by polygons are commonly agreed to be used in a majority of geometric scenarios [20]. The proposed CEF and CEF-DT can be applied for skeletonization. The skeletal points are the ones, where at least two distinct receptive fields have the same value [13]. In continuous case subtracting one receptive field from another will result in zero values for the skeletal points (see Table I, last row). The resulting skeleton preserves topological and geometrical information.

According to the Definition 5, and as observed in Section IV-C, the separating curves pass through the vertices of the polygon. This fact enables to efficiently remove some of the

spurious branches by excluding the separating curves between the neighboring line-seeds (see Figure 7).

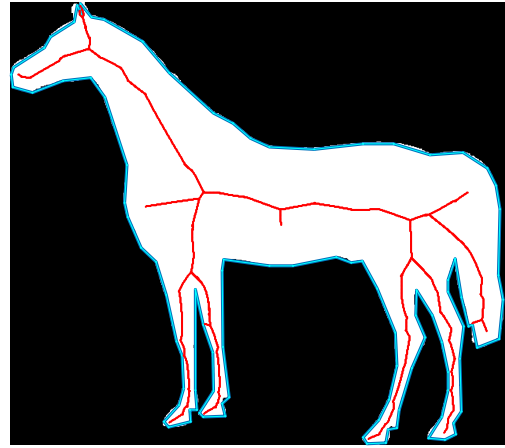


Fig. 7: CEF-based skeleton (red) of the horse that is approximated by 100 vertices (cyan) after removing the separating curves of the consecutive line-seeds.

In general, the produced skeleton is not MAT, i.e. its points are not equidistant from the borders of the shape. In contrast, the CEF-based skeleton is shifted towards the smaller edges. Thanks to the eccentricity, the seeds with comparably greater distance between its pixels have a greater receptive field in the resulting CEF-DT as compared to classical EDT (see Table I, columns 2-5).

The distance value at each skeletal point of MAT can be associated with the local thickness of the shape in terms of the maximal ball that is fit inside the shape boundary (see Fig. 8b). In contrast, the values of the CEF-based skeleton reflect the elongation of the shape. This can be shown on an example of the shape that is combined by the rectangles of the different length (see Fig. 8a).

The MAT can be obtained using the CEF in two cases: (1) seeds contain identical pixels (see Fig. 2), (2) line-seeds have the same length (see Table I, column 1).

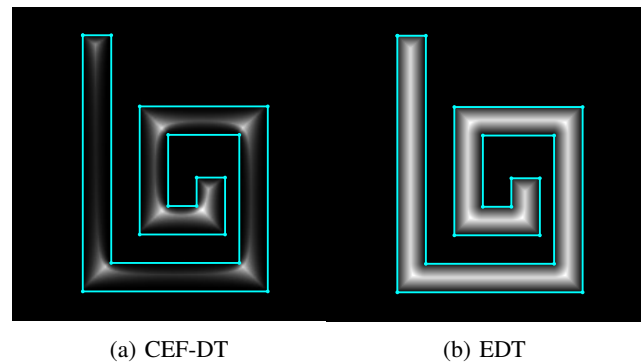
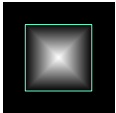
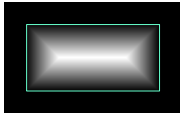
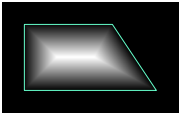
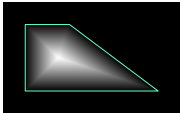
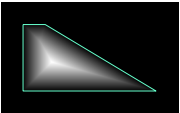
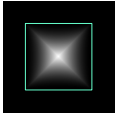
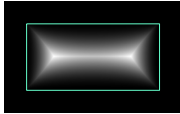
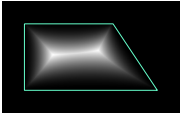
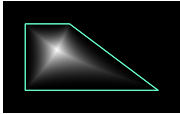
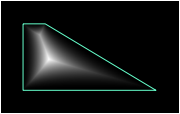
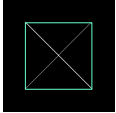
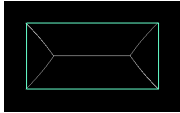
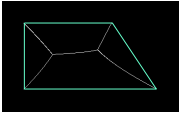
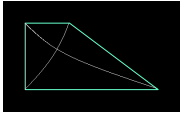
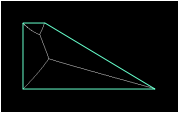


Fig. 8: Comparison of the distance fields produced by CEF-DT and EDT. The input polygonal shape is shown in cyan.



TABLE I: Comparison of the distance fields produced by traditional EDT and the proposed CEF-DT (first and second rows), and obtained skeleton (third row). The input polygonal shape is highlighted with cyan.

	1	2	3	4	5
EDT					
CEF-DT					
Skeleton from CEF-DT					

#### D. Parallel computing

The proposed algorithm for computing CEF-DT, as well as the skeletonization based on CEF-DT yield to parallelization. Indeed, for each element in seed set the distance field of CED values can be computed independently, whereas CEF-DT is a pixel-wise operation by definition. In case of skeletonization, distinct pairs of receptive fields can be processed in parallel.

#### VI. CONCLUSION

This paper presents a distance (CED) that is based on the properties of the confocal ellipses. This metric is then used to produce a new type of distance field - confocal elliptical field (CEF). For the discrete case, the proposed CED and CEF are redefined with relation to DT, and make it possible to efficiently compute a skeleton in a parallel way, that is consistent with the continuous case. As a special case, the proposed approach also enables to obtain the classical MAT.

The properties of the CEF enable to efficiently remove the spurious branches by grouping the seeds belonging to the same line, or by excluding the separating curves between the consecutive line-seeds.

CED computes the distance between a point and a line segment and extends the classical point to point measurements. Point and line segment are simplices of dimensions 0 and 1 respectively. There are ideas to go further and compute distances between simplices of higher order and simplicial complexes such as triangular meshes.

#### REFERENCES

- [1] G. Borgefors, "Distance transformations in digital images," *Computer vision, graphics, and image processing*, vol. 34, no. 3, pp. 344–371, 1986.
- [2] F. Malmberg, R. Strand, J. Zhang, and S. Sclaroff, "The boolean map distance: Theory and efficient computation," in *International Conference on Discrete Geometry for Computer Imagery*. Springer, 2017, pp. 335–346.
- [3] C. R. Maurer, R. Qi, and V. Raghavan, "A linear time algorithm for computing exact euclidean distance transforms of binary images in arbitrary dimensions," *IEEE Transactions on Pattern Analysis and Machine Intelligence*, vol. 25, no. 2, pp. 265–270, 2003.
- [4] K. C. Ciesielski, X. Chen, J. K. Udupa, and G. J. Grevera, "Linear time algorithms for exact distance transform," *Journal of Mathematical Imaging and Vision*, vol. 39, no. 3, pp. 193–209, 2011.
- [5] H. Talbot and B. Appleton, "Elliptical distance transforms and the object splitting problem," *Proceedings of ISMM2002*, pp. 229–240, 2002.
- [6] P. Saha, G. Borgefors, and G. Sanniti di Baja, "A survey on skeletonization algorithms and their applications," *Pattern Recognition Letters*, vol. 76, pp. 3–12, 2016.
- [7] H. Blum, "A transformation for extracting descriptors of shape," *Models for the Perception of Speech and Visual Form*, pp. 362–380, 1967.
- [8] P. Saha, G. Borgefors, and G. Sanniti di Baja, "Skeletonization: Theory, methods, and applications," 2017.
- [9] R. Ogniewicz and M. Ilg, "Voronoi skeletons: Theory and applications," in *Computer Vision and Pattern Recognition, 1992. Proceedings CVPR'92., 1992 IEEE Computer Society Conference on*. IEEE, 1992, pp. 63–69.
- [10] R. L. Ogniewicz and O. Kübler, "Hierarchic voronoi skeletons," *Pattern recognition*, vol. 28, no. 3, pp. 343–359, 1995.
- [11] T. K. Dey and W. Zhao, "Approximating the medial axis from the voronoi diagram with a convergence guarantee," *Algorithmica*, vol. 38, no. 1, pp. 179–200, 2004.
- [12] A. Bucksch and R. Lindenbergh, "Campinoa skeletonization method for point cloud processing," *ISPRS journal of photogrammetry and remote sensing*, vol. 63, no. 1, pp. 115–127, 2008.
- [13] R. Kimmel, D. Shaked, N. Kiryati, and A. M. Bruckstein, "Skeletonization via distance maps and level sets," *Computer vision and image understanding*, vol. 62, no. 3, pp. 382–391, 1995.
- [14] K. Siddiqi, S. Bouix, A. Tannenbaum, and S. W. Zucker, "Hamilton-jacobi skeletons," *International Journal of Computer Vision*, vol. 48, no. 3, pp. 215–231, 2002.
- [15] F. Leymarie and M. D. Levine, "Simulating the grassfire transform using an active contour model," *IEEE transactions on pattern analysis and machine intelligence*, vol. 14, no. 1, pp. 56–75, 1992.
- [16] X. Bai, L. J. Latecki, and W.-Y. Liu, "Skeleton pruning by contour partitioning with discrete curve evolution," *IEEE transactions on pattern analysis and machine intelligence*, vol. 29, no. 3, 2007.
- [17] D. Hilbert and S. Cohn-Vossen, "The cylinder, the cone, the conic sections, and their surfaces of revolution," in *Geometry and the imagination, 2nd ed.* New York: Chelsea Publishing Company, 1999, ch. 2, pp. 7–9.
- [18] G. Borgefors, "Distance transformations in hexagonal grids," in *Image Analysis and Processing II*. Springer, 1988, pp. 213–220.
- [19] R. Strand, "Minimal paths by sum of distance transforms," in *International Conference on Discrete Geometry for Computer Imagery*. Springer, 2016, pp. 349–358.
- [20] F. Aurenhammer, R. Klein, and D.-T. Lee, *Voronoi diagrams and Delaunay triangulations*. World Scientific Publishing Company, 2013.